ISSN 1023-1935, Russian Journal of Electrochemistry, 2020, Vol. 56, No. 2, pp. 118–123. © Pleiades Publishing, Ltd., 2020.
Russian Text © The Author(s), 2020, published in Elektrokhimiya, 2020, Vol. 56, No. 2, pp. 127–132.

ZrO_2–Sc_2O_3 Solid Electrolytes Doped with Yb_2O_3 or Y_2O_3[1]

E. E. Lomonova[a], D. A. Agarkov[b, c], M. A. Borik[a], G. M. Eliseeva[b], A. V. Kulebyakin[a], I. E. Kuritsyna[b], F. O. Milovich[d], V. A. Myzina[a], V. V. Osiko[a], A. S. Chislov[a, d], and N. Yu. Tabachkova[a, d, *]

[a] *Prokhorov Institute of General Physics, Russian Academy of Sciences, Moscow, 119991 Russia*
[b] *Institute of Solid State Physics, Russian Academy of Sciences, Chernogolovka, Moscow oblast, 142432 Russia*
[c] *Moscow Institute of Physics and Technology (National Research University), Dolgoprudnyi, Moscow oblast, 117303 Russia*
[d] *National University of Science and Technology MISiS, Moscow, 119049 Russia*
**e-mail: ntabachkova@gmail.com*

Received September 3, 2018; revised February 14, 2019; accepted July 10, 2019

Abstract—The effects of the Y_2O_3 and Yb_2O_3 co-doping impurities on the transport characteristics and stabilization of the cubic phase in solid solutions based on ZrO_2–Sc_2O_3 were compared. The crystals of the $(ZrO_2)_{0.99-x}(Sc_2O_3)_x(Yb_2O_3)_{0.01}$ and $(ZrO_2)_{0.99-x}(Sc_2O_3)_x(Y_2O_3)_{0.01}$ (x = 0.08–0.10) solid solutions were grown by directed crystallization of the melt in a cold container. The high-temperature cubic phase was stabilized at a total concentration of stabilizing oxides of 11 mol % for $(ZrO_2)_{0.99-x}(Sc_2O_3)_x(Y_2O_3)_{0.01}$ crystals and at 10 mol % for $(ZrO_2)_{0.99-x}(Sc_2O_3)_x(Yb_2O_3)_{0.01}$ crystals. At (9–10) mol % scandium oxide, the high-temperature conductivity of the crystals co-doped with ytterbium oxide was higher than in the case of the crystals co-doped with yttrium oxide. The $(ZrO_2)_{0.9}(Sc_2O_3)_{0.09}(Yb_2O_3)_{0.01}$ crystals have maximum conductivity over the whole temperature range.

Keywords: solid electrolytes, zirconia, single crystals, phase composition, structure, ionic conductivity
DOI: 10.1134/S1023193520020081

INTRODUCTION

The materials based on ZrO_2–Sc_2O_3 solid solutions used in solid oxide fuel cells (SOFCs) are of great interest because they have the highest ion conductivity among solid electrolytes based on zirconia [1–4]. The use of these materials allows the working temperature of the fuel cell to be reduced to 800°C, which is very important for increasing the stability, service life, and reliability of electrochemical devices. For composites with the maximum conductivity ZrO_2–(9–11) mol % Sc_2O_3, however, there are some problems in their application as materials for electrolytic membranes: instability of transport characteristics at working temperatures and transition of rhombohedral to cubic phase on heating. One possible way to solve these problems is stabilization of the highly conductive cubic phase by co-doping the ZrO_2–Sc_2O_3 solid solutions with yttria or rare earth oxides [5–10]. The co-doping impurity is chosen such that a stable single-phase cubic solid solution should be obtained in the temperature range from room to working temperature (700–1000°C) and the high conductivity typical of the ZrO_2–Sc_2O_3 system should be maintained.

The effect of the ionic radius of rare-earth oxides on oxygen-ion conductivity was studied in many works [11–13]. It was shown that the activation energy, which determines the conductivity, is the sum of migration and association energies in the low-temperature range (below 600–700°C) and is determined by migration energy in the high-temperature range. These values depend on the radius of the dopant ion.

The goal of this study was to synthesize the crystals of the ZrO_2–Sc_2O_3 solid solutions co-doped with yttrium or ytterbium oxides, examine their transport characteristics, and compare the effects of the Y_2O_3 and Yb_2O_3 co-doping impurities on the transport characteristics and stabilization of the cubic phase in ZrO_2–Sc_2O_3 solid solutions.

EXPERIMENTAL

The crystals of the $(ZrO_2)_{0.99-x}(Sc_2O_3)_x(Yb_2O_3)_{0.01}$ and $(ZrO_2)_{0.99-x}(Sc_2O_3)_x(Y_2O_3)_{0.01}$ solid solutions (x = 0.08–0.10) were grown by directed crystallization of the melt in a cold container [14].

[1] Published on the basis of materials of the 5th All-Russia Conference "Fuel Cells and Power Plants Based on Them" (with international participation), Suzdal, 2018.

Table 1. Phase composition, notation, and density of the grown crystals

Composite	Symbol	Phase composition*	Density, g/cm^3
$(ZrO_2)_{0.91}(Sc_2O_3)_{0.08}(Yb_2O_3)_{0.01}$	8Sc1YbSZ	t-ZrO_2	5.924 ± 0.001
$(ZrO_2)_{0.91}(Sc_2O_3)_{0.08}(Y_2O_3)_{0.01}$	8Sc1YSZ	t-ZrO_2	5.824 ± 0.001
$(ZrO_2)_{0.90}(Sc_2O_3)_{0.09}(Yb_2O_3)_{0.01}$	9Sc1YbSZ	c-ZrO_2	5.863 ± 0.001
$(ZrO_2)_{0.90}(Sc_2O_3)_{0.09}(Y_2O_3)_{0.01}$	9Sc1YSZ	t-ZrO_2 c-ZrO_2	5.769 ± 0.001
$(ZrO_2)_{0.89}(Sc_2O_3)_{0.10}(Yb_2O_3)_{0.01}$	10Sc1YbSZ	r-ZrO_2 c-ZrO_2	5.820 ± 0.001
$(ZrO_2)_{0.89}(Sc_2O_3)_{0.10}(Y_2O_3)_{0.01}$	10Sc1YSZ	c-ZrO_2	5.744 ± 0.001

* t is the tetragonal modification of ZrO_2, c is its cubic modification, and r is its rhombohedral modification.

The chemical composition of the grown crystals was determined using a JEOL 5910 LV scanning electron microscope with an INCA Energy energy dispersive attachment. When measuring the crystal composition, fused zirconium, scandium, yttrium, and ytterbium oxides were used as standards. The crystals were analyzed by X-ray diffractometry on a Bruker D8 diffractometer (CuK_α radiation) and Raman spectroscopy. A laser with a wavelength of 532 nm was used as an excitation source. The unit for studying the Raman spectra of the crystals in an air atmosphere at room temperature and working temperatures of up to 1000°C was described in detail in previous works [15–17].

The density was determined by hydrostatic weighing on a Sartorius device for hydrostatic weighing.

The conductivity of the crystals based on zirconia was studied in the temperature range 400–900°C using a Solartron SI 1260 frequency response analyzer in the frequency range 1 Hz–5 MHz with an AC signal amplitude of 24 mV. Plates with an area of 7 × 7 mm^2 and a thickness of 0.5 mm were used for measurements. To form current contacts, a platinum paste was applied to opposite sides of the crystals and burnt in at 950°C for 1 h in air. The measurements were performed in a heating mode at a step of 50°C and exposure at this temperature until thermal equilibrium was reached. The impedance spectra were processed using the ZView program (ver. 2.8). The specific conductivity of the crystals was calculated from the data obtained by processing the impedance spectra, taking into account the dimensions of the samples.

RESULTS AND DISCUSSION

Table 1 shows the compositions of the solid solutions, notation used below, phase composition, and crystal density. The grown crystals had a shape and size similar to those of the zirconia crystals stabilized with scandium and/or yttrium oxide obtained in a cold crucible [18, 19].

The 8Sc1YbSZ and 8Sc1YSZ crystals were homogeneous and turbid and had no visible defects. When the Sc_2O_3 concentration in the solid solutions increased to 9 and 1 mol % Y_2O_3 was added, transparent regions appeared in the crystals. The transparent regions were in the lower part of the 9Sc1YSZ crystal, which corresponded to the start of crystallization, and semitransparent (cloudy) regions were located in the upper part of the crystal (the end of crystallization). In some 9Sc1YSZ crystals, alternating transparent and cloudy regions could be seen in the central part of the crystallized melt ingot. Transparent single crystals having no visible defects and additionally doped with 1 mol % Y_2O_3 were obtained only at a concentration of 10 mol % Sc_2O_3 in the solid solution.

The doping of the ZrO_2–(9 mol %) Sc_2O_3 solid solution with 1 mol % Yb_2O_3 led to the formation of transparent homogeneous single crystals unlike the situation with the 9Sc1YSZ crystals. When the Sc_2O_3 concentration increased to 10 mol % in the solid solutions doped with 1 mol % Yb_2O_3, opalescent crystals with microcracks in the ingots were obtained.

The phase composition of the crystals additionally doped with 1 mol % Y_2O_3 changed from tetragonal to cubic at increased Sc_2O_3 concentration. Thus, the 8Sc1YSZ crystals contained only the tetragonal modification of ZrO_2. The images of the microstructure obtained in transmitted light showed twins on the polished thin plates, which formed during the cubic-to-tetragonal transition when the single crystal was cooled in accordance with the phase diagram of ZrO_2–Sc_2O_3. Due to the presence of light-scattering twins, the tetragonal crystals of 8Sc1YSZ were cloudy and opaque. According to the XRD data, the 9Sc1YSZ crystals were two-phase and contained regions with a tetragonal and cubic structure. The 10Sc1YSZ crystals were single-phase with a cubic fluorite structure.

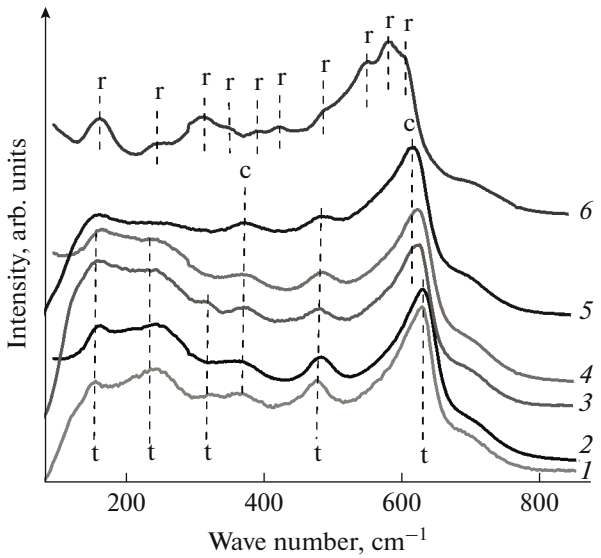

Fig. 1. Raman spectra of the $(ZrO_2)_{0.99-x}(Sc_2O_3)_x(Y_2O_3)_{0.1}$ and $(ZrO_2)_{0.99-x}(Sc_2O_3)_x(Yb_2O_3)_{0.1}$ crystals: (*1*) 8Sc1YSZ, (*2*) 8Sc1YbSZ, (*3*) 9Sc1YSZ, (*4*) 9Sc1YbSZ, (*5*) 10Sc1YSZ, and (*6*) 10Sc1YbSZ.

The phase composition of the crystals additionally doped with 1 mol % Yb_2O_3 also changed depending on the Sc_2O_3 concentration. The 8Sc1YbSZ crystals were tetragonal, 9Sc1YbSZ were cubic, and 10Sc1YbSZ contained the cubic and rhombohedral modifications of zirconia.

The crystal density depends on both the type and concentration of the stabilizing oxide and on the phase composition of the crystal. At the same Sc_2O_3 concentration in crystals, the density of the crystals co-doped with Yb_2O_3 is higher than that of the crystals additionally doped with Y_2O_3 because the mass-to-volume ratio of Yb^{3+} ions is higher than that of Y^{3+} ions. The crystal density decreases when the Sc_2O_3 concentration in the crystals doped with 1 mol % Yb_2O_3 increases. The highest density was inherent in the crystals containing the tetragonal 8Sc1YbSZ phase. The density of the cubic crystals is lower than that of the tetragonal ones. For these crystals, it is lower than for the 9Sc1YbSZ single-phase cubic single crystals because of the presence of the rhombohedral phase regions in 10Sc1YbSZ.

In the crystals additionally doped with 1 mol % Y_2O_3, the crystal density also decreases with increasing Sc_2O_3 concentration, which is associated with a change in the phase composition in these crystals from tetragonal (8Sc1YSZ) to cubic (10Sc1YSZ) solid solution based on zirconia.

Thus, the high-temperature cubic phase is stabilized at a total concentration of stabilizing oxides of 11 mol % for the ScYSZ crystals and 10 mol % for the Sc1YbSZ crystals. Despite the smaller ionic radius of Yb^{3+} compared to that of Y^{3+}, stabilization of the cubic phase in the crystals co-doped with Yb_2O_3 occurs at lower Sc_2O_3 concentrations in solid solution than in the crystals co-doped with Y_2O_3.

In the ZrO_2–R_2O_3 binary systems, the decrease in the ionic radius lowers the temperature of the transition from the high-temperature cubic phase to the low-temperature tetragonal phase, which leads to the conservation of the high-temperature cubic phase at room temperature at lower concentrations of the stabilizing oxide. This regularity is possibly also valid for the ternary systems under study.

The phase composition was also studied by Raman scattering. Figure 1 shows the Raman spectra of the crystals under study.

The Raman spectra of the 8Sc1YSZ and Sc1YbSZ crystals contain the peaks characteristic of the tetragonal phase [20, 21]. In the Raman spectra of the 9Sc1YSZ crystals, the lines are substantially broadened due to the presence of the cubic and tetragonal phases in these crystals. The Raman spectra of the 10Sc1YbSZ crystals contain the lines corresponding to the rhombohedral phase [21], which are also substantially broadened possibly because of the presence of the cubic phase in these crystals.

The spectra of the 9Sc1YbSZ and 10Sc1YSZ crystals are similar and contain the 480 cm^{-1} band in addition to the lines of the cubic phase, which was attributed to the tetragonal t" phase in [22–24]. The degree of tetragonality of this phase is $c/\sqrt{2}a = 1$, but the phase belongs to the symmetry group $P42/nmc$ because of the displacement of oxygen ions in the anion sublattice [23]. The Raman spectra characteristic of the t-ZrO_2, t"-ZrO_2, and c-ZrO_2 phases were given in [25].

Thus, the crystal structure, which was identified by XRD analysis as a cubic structure, is a tetragonal t" phase according to the Raman data.

Figure 2 presents the temperature dependences of specific conductivity for all the crystals under study in Arrhenius coordinates. Figure 3 shows the impedance spectra for the 10Sc1YSZ and 10Sc1YbSZ crystals as an example.

The temperature dependence of specific conductivity for the 10Sc1YbSZ crystals in the temperature range 450–550°C shows an inflection that is due to the phase transition of the rhombohedral phase into the cubic phase. The highest conductivity is inherent in the 9Sc1YbSZ crystals and the lowest in the 8Sc1YbSZ crystals over the whole temperature range.

Figure 4 shows the dependence of the conductivity of the Sc1YbSZ and Sc1YSZ crystals on the Sc_2O_3 content. According to Fig. 4, an increase in the Sc_2O_3 content in the crystals co-doped with yttrium or ytterbium oxides leads to an increase in their conductivity. For the crystals doped with Yb_2O_3, the concentration

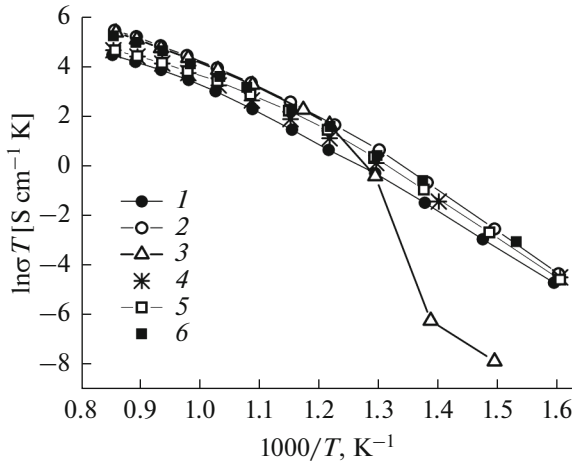

Fig. 2. Temperature dependences of the bulk conductivity of the $(ZrO_2)_{0.99-x}(Sc_2O_3)_x(Y_2O_3)_{0.1}$ and $(ZrO_2)_{0.99-x}(Sc_2O_3)_x(Yb_2O_3)_{0.1}$ crystals: (*1*) 8Sc1YbSZ, (*2*) 9Sc1YbSZ, (*3*) 10Sc1YbSZ, (*4*) 8Sc1YSZ, (*5*) 9Sc1YSZ, and (*6*) 10Sc1YSZ.

dependence has a maximum at 9 mol % Sc_2O_3. In the case of co-doping with Y_2O_3, the conductivity appreciably increased only at 10 mol % Sc_2O_3. The observed concentration dependences of conductivity can be explained if we take into account the data on the phase composition of the samples. Thus, for the 8Sc1YbSZ and 8Sc1YSZ single-phase tetragonal crystals, as well as for the 9Sc1YSZ two-phase crystal, which is a mixture of the tetragonal and cubic phases, the conductivity is ~0.1 S/cm. Similar conductivity values were obtained for the undoped 8ScSZ and 9ScSZ tetragonal crystals [26]. The 9Sc1YbSZ crystals are single-phase pseudocubic (t" phase) and have the maximum conductivity. When the Sc_2O_3 content increases to 10 mol % (10Sc1YbSZ crystal), regions of rhombohedral phases appear in the crystals, and their conductivity decreases. The 10Sc1YSZ crystals are also single-phase pseudocubic (t" phase), but their conductivity is lower than that of the 9Sc1YbSZ crystals, which have a similar crystal structure. This difference in conductivity can be due to the large ionic radius of Y^{3+} compared to that of Yb^{3+}. The introduction of a larger ion during heterovalent substitution leads to an increase in stresses in the lattice, which decrease the conductivity. In addition, the 10Sc1YSZ and 9Sc1YbSZ crystals differ in the total concentration of stabilizing oxides (11 and 10 mol %, respectively). An increase in the total concentration of stabilizing oxides above a certain threshold value, which depends on the type of the stabilizing impurity, leads to a decrease in the conductivity due to the formation of clusters of oxygen vacancies and dopant cations [11].

Note that the conductivity of the 9Sc1YbSZ crystals at 900°C (0.214 S/cm) is comparable to that of the 10ScSZ crystals (0.197 S/cm) [26]. Unlike the 10ScSZ

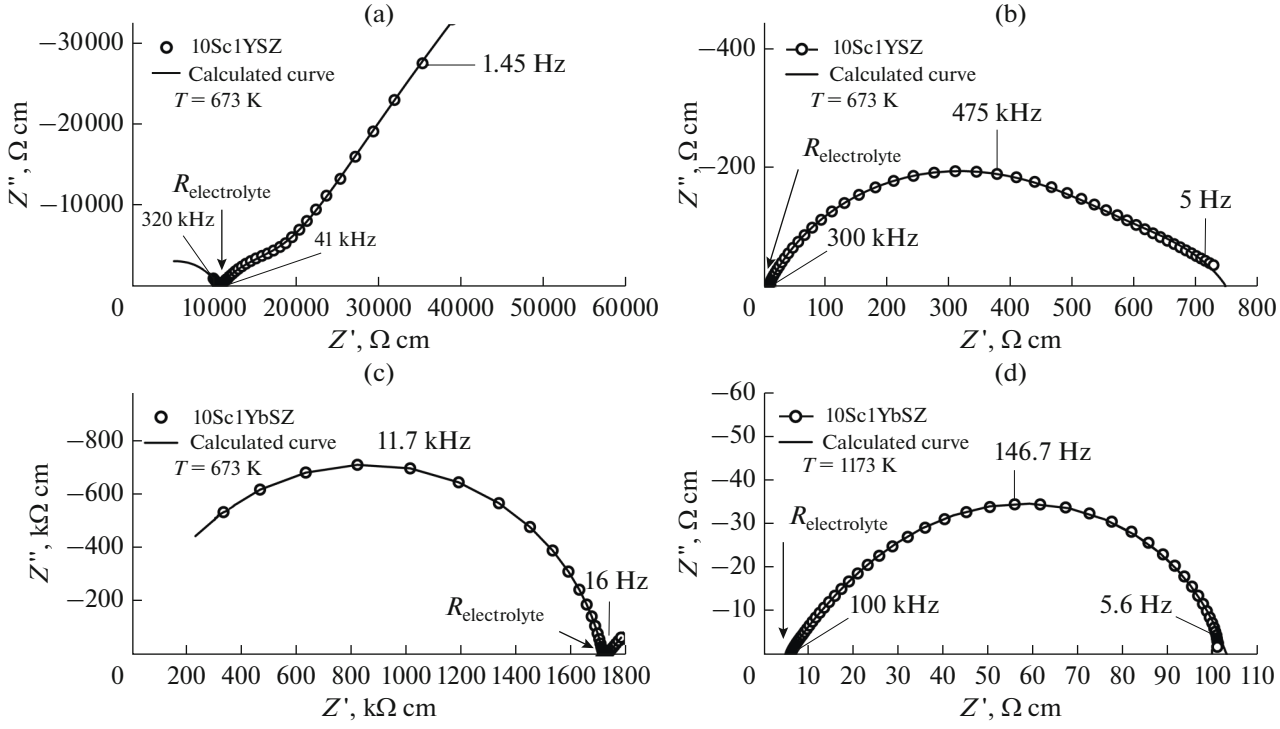

Fig. 3. Impedance spectra of the (a), (b) 10Sc1YSZ and (c), (d) 10Sc1YbSZ crystals at 673 and 1173 K.

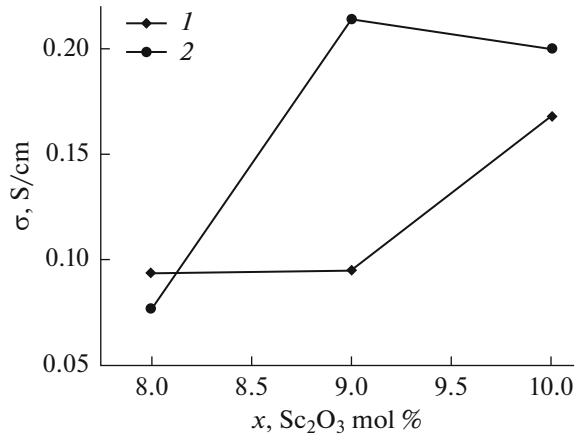

Fig. 4. Comparison of the ion conductivities of the crystals at 900°C: (*1*) $(ZrO_2)_{0.99-x}(Sc_2O_3)_x(Y_2O_3)_{0.1}$ and (*2*) $(ZrO_2)_{0.99-x}(Sc_2O_3)_x(Yb_2O_3)_{0.1}$.

crystal containing the rhombohedral phase, however, the 9Sc1YbSZ sample is single-phase pseudocubic.

CONCLUSIONS

A comparative study of the phase composition and transport characteristics of the crystals of the $(ZrO_2)_{0.99-x}(Sc_2O_3)_x(Yb_2O_3)_{0.1}$ and $(ZrO_2)_{0.99-x}(Sc_2O_3)_x(Y_2O_3)_{0.1}$ solid solutions (x = 0.08–0.10) obtained by directed crystallization of the melt in a cold container was performed.

It was shown that the pseudocubic (t" phase) was stabilized at a total concentration of stabilizing oxides of 11 mol % for the ScYSZ crystals and 10 mol % for the Sc1YbSZ crystals.

It was found that the crystal conductivity increased with the Sc_2O_3 concentration for all the compositions under study. For the crystals co-doped with yttrium and ytterbium oxide, the maximum conductivity was observed at different Sc_2O_3 contents (10 and 9 mol %, respectively). At 9–10 mol % Sc_2O_3, the high-temperature conductivity of the crystals co-doped with Yb_2O was higher than in the case of the crystals doped with Y_2O_3. The maximum conductivity was inherent in the 9Sc1YbSZ crystals over the whole temperature range.

FUNDING

This study was financially supported by the Russian Scientific Foundation (project no. 16-13-00056 "Development of materials science fundamentals and creation of highly efficient oxygen-conducting membranes for solid oxide fuel cells").

CONFLICT OF INTEREST

The authors declare that they have no conflict of interest.

REFERENCES

1. Badwal, S.P.S., Ciacchi, F.T., and Milosevic, D., Scandia–zirconia electrolytes for intermediate temperature solid oxide fuel cell operation, *Solid State Ionics*, 2000, vol. 136, p. 91.
2. Kumar, A., Jaiswal, A., Sanbui, M., and Omar, S., Oxygen-ion conduction in scandia-stabilized zirconia-ceria solid electrolyte (xSc_2O_3–$1CeO_2$–$(99-x)ZrO_2$, $5 \le x \le 11$), *J. Am. Ceram. Soc.*, 2016, p. 1.
3. Stricker, D.W. and Carlson, W.G., Electrical conductivity in the ZrO_2-rich region of several M_2O_3–ZrO_2 systems, *J. Am. Ceram. Soc.*, 1965, vol. 48, p. 286.
4. Borik, M.A., Bredikhin, S.I., Kulebyakin, A.V., Kuritsyna, I.E., Lomonova, E.E., Milovich, F.O., Myzina, V.A., Osiko, V.V., Panov, V.A., Ryabochkina, P.A., Seryakov, S.V., and Tabachkova, N.Yu., Melt growth, structure and properties of $(ZrO_2)_{1-x}(Sc_2O_3)_x$ solid solution crystals (x = 0.035–0.11), *J. Cryst. Growth*, 2016, vol. 443, p. 54.
5. Yamamura, H., Matsusita, T., Nishino, H., and Kakinuma, K., Co-doping effect on electrical conductivity in the fluorite-type solid-solution systems $Zr_{0.7}(Sc_{1-x}M_x)_{0.3}O_{2-\delta}$ (M = Ca, Mg, Al, Gd, Yb), *J. Mater. Sci.: Mater. Electron.*, 2002, vol. 13, p. 57.
6. Lee, D.-S., Kim, W.S., Choi, S.H., Kim, J., Lee, H.-W., and Lee, J.-H. Characterization of ZrO_2 co-doped with Sc_2O_3 and CeO_2 electrolyte for application of intermediate temperature SOFCs, *Solid State Ionics*, 2005, vol. 176, p. 33.
7. Omar, S., Najib, W.B., Chen, W., and Bonanos, N., Electrical conductivity of 10 mol % Sc_2O_3–1 mol % M_2O_3–ZrO_2 ceramics, *J. Am. Ceram. Soc.*, 2012, vol. 95, p. 1965.
8. Chiba, R., Ishii, T., and Yoshimura, F., Temperature dependence of ionic conductivity in $(1-x)ZrO_{2-(x-y)}$ $Sc_2O_{3-y}Yb_2O_3$ electrolyte material, *Solid State Ionics*, 1996, vol. 91, p. 249.
9. Spirin, A. Ivanov, V., Nikonov, A., Lipilin, A., Paranin, S., Khrustov, V., and Spirina A., Scandia-stabilized zirconia doped with yttria: Synthesis, properties, and ageing behavior, *Solid State Ionics*, 2012, vol. 225, p. 448.
10. Omar, S. and Bonanos, N., Ionic conductivity ageing behaviour of 10 mol % Sc_2O_3–1 mol % CeO_2–ZrO_2 ceramics, *J. Mater. Sci.*, 2010, vol. 45, p. 6406.
11. Arachi, Y., Sakai, H., Yamamoto, O., Takeda, Y., and Imanishai, N., Electrical conductivity of the ZrO_2–Ln_2O_3 (Ln-lanthanides) system, *Solid State Ionics*, 1999, vol. 121, p. 133.
12. Kilner, J.A. and Brook, R.J., A study of oxygen ion conductivity in doped non-stoichiometric oxides, *Solid State Ionics*, 1982, vol. 6, p. 237.
13. Zacate, M.O., Minervini, L., Bradfield, D.J., Grimes, R.W., and Sickafus, K.E., Defect cluster formation in M_2O_3 doped cubic ZrO_2, *Solid State Ionics*, 2000, vol. 128, p. 243.
14. Osiko, V.V., Borik, M.A., and Lomonova, E.E., *Synthesis of refractory materials by skull melting technique,*

Springer Handbook of Crystal Growth, 2010, Part B, p. 433.

15. Agarkov, D.A., Burmistrov, I.N., Tsybrov, F.M., Tartakovskii, I.I., Kharton, V.V., and Bredikhin, S.I., In-situ Raman spectroscopy analysis of the interfaces between Ni-based SOFC anodes and stabilized zirconia electrolyte, *Solid State Ionics,* 2017, vol. 302, p. 133.
16. Agarkov, D.A., Burmistrov, I.N., Tsybrov, F.M., Tartakovskii, I.I., Kharton, V.V., and Bredikhin, S.I., Kinetics of NiO reduction and morphological changes in composite anodes of solid oxide fuel cells: Estimate using Raman scattering technique, *Russ. J. Electrochem.,* 2016, vol. 52, p. 600.
17. Agarkov, D.A., Burmistrov, I.N., Tsybrov, F.M., Tartakovskii, I.I., Kharton, V.V., Bredikhin, S.I., and Kveder, V.V., Analysis of interfacial processes at the SOFC electrodes by in-situ Raman spectroscopy, *ECS Trans.,* 2015, vol. 68(1), p. 2093.
18. Borik, M.A., Bredikhin, S.I., Bublik, V.T., Kulebyakin, A.V., Kuritsyna, I.E., Lomonova, E.E., V.A., Osiko, V.V., Ryabochkina, P.A., Seryakov, S.V., and Tabachkova, N.Yu., Phase composition, structure and properties of $(ZrO_2)_{1-x-y}(Sc_2O_3)_x(Y_2O_3)_y$ solid solution crystals (x = 0.08–0.11; y = 0.01–0.02) grown by directional crystallization of the melt, *J. Cryst. Growth*, 2017, vol. 457, p. 122.
19. Borik, M.A., Bredikhin, S.I., Bublik, V.T., Kulebyakin, A.V., Kuritsyna, I.E., Lomonova, E.E., Milovich, Ph.O., Myzina, V.A., Osiko, V.V., Ryabochkina, P.A., and Tabachkova, N.Y., Structure and conductivity of yttria and scandia-doped zirconia crystals grown by skull melting, *J. Am. Ceram. Soc.*, 2017, vol. 100, p. 5536.
20. Fujimori, H., Yashima, M., Kakihana, M., and Yoshimura, M., Structural changes of scandia-doped zirconia solid solutions: Rietveld analysis and Raman scattering, *J. Am. Ceram. Soc.,* 1998, vol. 81, p. 2885.
21. Fujimori, H., Yashima, M., Kakihana, M., and Yoshimura M., β-cubic phase transition of scandia-doped zirconia solid solution: Calorimetry, X-ray diffraction, and Raman scattering, *J. Appl. Phys.*, 2002, vol. 91, p. 6493.
22. Yashima, M., Sasaki, S., Kakihana, M., Yamaguchi, Y., Arashi, H., and Yoshimura, M., Oxygen-induced structural change of the tetragonal phase around the tetragonal-cubic phase-boundary in ZrO_2–$YO_{1.5}$ solid-solutions, *Acta Crystallogr., Sect. B: Struct. Sci.*, 1994, vol. 50, p. 663.
23. Yashima, M., Ohtake, K., Kakihana, M., Arashi, H., and Yoshimura, M., Determination of tetragonal-cubic phase boundary of $Zr_{1-x}R_xO_{2-x/2}$ (R = Nd, Sm, Y, Er and Yb) by Raman scattering, *J. Phys. Chem. Solids*, 1996, vol. 57, p. 17.
24. Lipkin, D.M., Krogstad, J.A, Gao, Y., Johnson, C.A., Nelson, W.A., and Levi, C.G., Phase evolution upon aging of air plasma spray t'-zirconia coatings: I—synchrotron X-ray diffraction, *J. Am. Ceram. Soc.*, 2013, vol. 96, p. 290.
25. Hemberger, Y., Wichtner, N., Berthold, Ch., and Nickel, K.G., Quantification of yttria in stabilized zirconia by Raman spectroscopy, *Int. J. Appl. Ceram. Technol.*, 2016, vol. 13, p. 116.
26. Agarkov, D.A., Borik, M.A., Bublik, V.T., Bredikhin, S.I., Chislov, A.S., Kulebyakin, A.V., Kuritsyna, I.E., Lomonova, E.E., Milovich, F.O., Myzina, V.A., Osiko, V.V., and Tabachkova, N.Yu., Structure and transport properties of melt grown Sc_2O_3 and CeO_2 doped ZrO_2 crystals, *Solid State Ionics*, 2018, vol. 322, p. 24.

Translated by L. Smolina